Lithos 362–363 (2020) 105493

Contents lists available at ScienceDirect

Lithos

journal homepage: www.elsevier.com/locate/lithos

Research Article

Geochemistry and petrogenesis of Quaternary basalts from Weizhou Island, northwestern South China Sea: Evidence for the Hainan plume

Yu Zhang [a,b,c], Kefu Yu [a,b,c,*], Tianlai Fan [a,b,c], Yuanfu Yue [a,b,c], Rui Wang [a,b,c], Wei Jiang [a,b,c], Shendong Xu [a,b,c], Yinghui Wang [a,b,c]

[a] School of Marine Sciences, Guangxi University, Nanning 530004, PR China
[b] Guangxi Laboratory on the Study of Coral Reefs in the South China Sea, Guangxi University, Nanning 530004, PR China
[c] Coral Reef Research Center of China, Guangxi University, Nanning 530004, PR China

ARTICLE INFO

Article history:
Received 11 November 2019
Received in revised form 23 January 2020
Accepted 18 March 2020
Available online 20 March 2020

Keywords:
Weizhou Island
Quaternary basaltic volcanism
Hainan mantle plume
South China Sea
Mantle source

ABSTRACT

Weizhou Island, located in the northwestern South China Sea (SCS), is the largest volcanic island in China. Its eruption represents the most recent volcanic activity in and around the SCS. We determined whole-rock major- and trace-element contents and Hf–Sr–Nd–Pb isotope compositions of Quaternary basalts from Weizhou Island to provide insights into the nature of their mantle sources and formation processes. These basalts have SiO_2 contents of 48.21 to 50.04 wt% and belong to the alkaline series. The basalts bear the signature of typical ocean-island basalt, being characterized by enrichments in large-ion lithophile and high-field-strength elements, clear differentiation of light rare-earth elements (REEs) from heavy REEs ($(La/Yb)_N$ = 15.19–19.29, mean of 16.82), and show no obvious Eu anomalies (Eu/Eu^* = 0.98–1.17, mean of 1.04). Hf–Sr–Nd–Pb isotope compositions show that the mantle source of these basalts can be regarded as a mixture of a depleted MORB mantle source and enriched mantle 2 (EM2), with geochemical data supporting an origin of the EM2 end-member from the Hainan mantle plume. Combining the new results with previous findings, we propose that Cenozoic intraplate volcanism in the SCS and surrounding areas is related to the magmatic activity of a large igneous province and that this province is associated with the Hainan mantle plume.

1. Introduction

The South China Sea (SCS) is one of the largest marginal sea basins in the western Pacific. Although the SCS basin is small and young, the SCS has undergone almost a complete Wilson cycle (Zhang et al., 2018a, 2020). Therefore, the SCS is regarded as a natural laboratory for studying the evolution of continental margins, ocean-basin spreading, and other lithospheric processes.

Volcanic rocks can be used to elucidate deep processes in Earth's interior. Volcanic rocks in the SCS and surrounding areas provide clues to the Cenozoic evolution of the SCS ocean basin. Li et al. (2014) reported that opening of the SCS started at 33 Ma and ended at 15 Ma. Subsequently, Cenozoic intraplate volcanism became widespread in both the SCS basin and surrounding areas, including the Beibu Gulf, the Pearl River Mouth Basin (PRMB), and the Indochina block. Post-spreading volcanism in the SCS and surrounding areas has been divided into two magmatic series: the tholeiitic series (16–8 Ma) and the alkali series (<8 Ma) (Li et al., 2013; Shi and Yan, 2011). However, the magmatic origin of SCS volcanism is debated. Previous petrological and geochemical studies have proposed that the mantle source of the Cenozoic basalts in the SCS and surrounding areas is a mixture of depleted MORB mantle (DMM) and enriched mantle type 2 (EM2) (An et al., 2017; Jia et al., 2003; Yan et al., 2008, 2014, 2015, 2018; Yang and Fang, 2015; Zhang et al., 2018b). However, the origin of EM2 remains unresolved. Some researchers have suggested that the enriched components of the late Cenozoic volcanism originated from subcontinental lithospheric mantle (SCLM) (Tu et al., 1992a, 1992b; Hoang et al., 1996; Fan et al., 2008; Wang et al., 2012a; Huang et al., 2013; Ren et al., 2013), whereas others have proposed that these enriched components are related to the Hainan mantle plume (An et al., 2017; Li et al., 2013; Liu et al., 2017; Yan et al., 2008, 2015, 2018, 2019; Zhang et al., 2018b; Zou and Fan, 2010).

Weizhou Island in the Beibu Gulf is the largest and youngest Quaternary volcanic oceanic island in China (Fig. 1). Previous studies have used traditional isotope methods (Sr–Nd–Pb) to identify the source region(s) of the Weizhou Island basalts. Fan et al. (2008) showed that the Quaternary basaltic rocks on Weizhou Island are dissimilar to ocean-island basalt (OIB) and mid-ocean ridge basalt (MORB), and proposed that the EM2 component was derived from SCLM. In contrast, Li et al. (2013) suggested that the EM2 of late Cenozoic basalt in the Beibu

* Corresponding author at: School of Marine Sciences, Guangxi University, Nanning 530004, PR China.
E-mail address: kefuyu@scsio.ac.cn (K. Yu).

https://doi.org/10.1016/j.lithos.2020.105493
0024-4937/

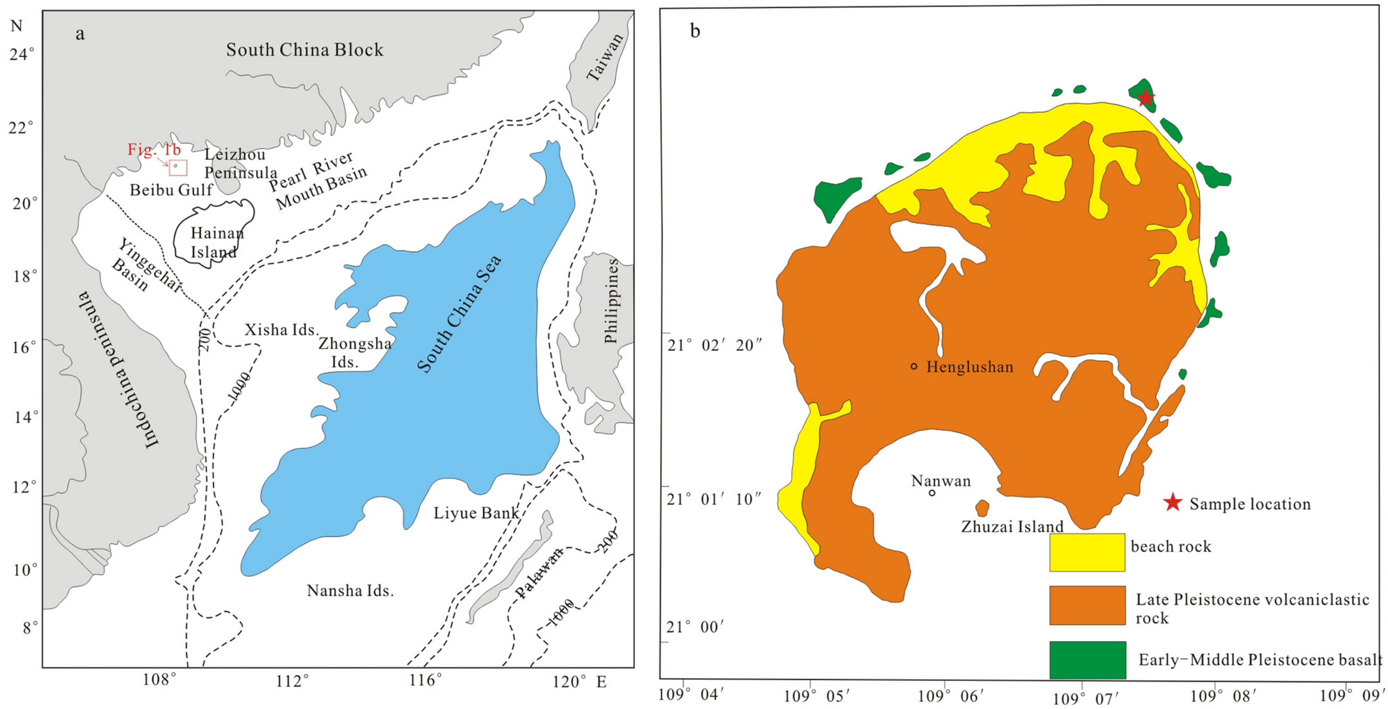

Fig. 1. (a) Location map of the South China Sea and surrounding area. (b) Sketch geological map of Weizhou Island (modified from Liu et al., 2017).

Gulf originated from the Hainan mantle plume. These results indicate that traditional Sr–Nd–Pb isotopic tracers are limited in their ability to discriminate SCLM from plume-influenced mantle. Consequently, additional geological methods are needed to resolve the origin of the Weizhou Island basalts. An et al. (2017) proposed that the combination of Hf isotope ratios with Sr–Nd–Pb isotope ratios can be used to distinguish between SCLM and plume-type signatures.

During a study of coral reefs at Weizhou Island, we recovered several cores and obtained fresh basalt samples from the northern margin of the island. In this study, we present new Hf isotope and Sr–Nd–Pb isotope compositions of these basalts to elucidate the nature of mantle sources and deep mantle geodynamic processes that led to the formation of these volcanic rocks, and discuss the implications for the magmatic evolution of the SCS and surrounding areas.

2. Geological setting and sample descriptions

The Beibu Gulf, located on the northwestern margin of the SCS, is a semi-enclosed gulf surrounded by the Leizhou Peninsula, Hainan Island, and the Indochina Peninsula (Fig. 1a). Tectonically, the gulf is situated at the intersection of the Pacific, India–Australia, and Eurasian plates, and belongs to the South China block (Huang and Li, 2007; Jia et al., 2003; Zhu et al., 2002). The northern margin of the SCS has been influenced by Pacific Plate subduction during the Mesozoic and rifting during the Cenozoic (Zhang et al., 2016a). During the Cenozoic, the northern margin of the SCS has gradually evolved from an active margin to a magma-poor margin (Zhu et al., 2012; Li et al., 2013; Gao et al., 2015, 2016). As a result of the extrusion of the Indochina block and seafloor spreading in the SCS, intensive magmatic and tectonic activity has occurred on the northern margin of the SCS (Zhang et al., 2016a).

More than 100 Cenozoic volcanoes are distributed across the Beibu Gulf and surrounding areas, forming the largest collection of Cenozoic volcanic rocks in South China. These volcanoes are found in or near deep fault zones and are controlled by the faults (Li et al., 2006). Weizhou Island is located in the Beibu Gulf Sea and has an area of 25 km^2. The volcanic activity on Weizhou Island has been divided into two stages: early–middle Pleistocene (1.42–0.49 Ma) and late Pleistocene (36–33 ka) (Fan et al., 2006, 2008) (Fig. 1b). Early–middle Pleistocene flood basalts are the products of the largest volcanic eruption on Weizhou Island. Henglushan Guogailing is a 52-m-high highland that is speculated to be the preserved top of the Pleistocene volcano (Fan et al., 2006, 2008). Lava from the Henglushan Guogailing volcanic center flooded the island, forming a shield-like shape. Much of the volcanic mass of the island is beneath sea level. During the late Pleistocene volcanic stage, phreato-magmatic eruptions formed typical maars and thick deposits that covered most of Weizhou Island. After a long period of marine erosion, the modern landscape was formed (Fan et al., 2006, 2008; Huang and Li, 2007).

The samples analyzed during this study represent the first (early–middle Pleistocene) stage of volcanism. The rocks are black-gray in color and show intergranular and local porphyritic textures. The samples are composed primarily of varying proportions of plagioclase,

Table 1
Major-element compositions for Quaternary basalts from Weizhou Island, northwestern South China Sea.

	SiO_2	TiO_2	Al_2O_3	TFe_2O_3	MnO	MgO	CaO	Na_2O	K_2O	P_2O_5	LOI	Total	Mg#
GS2–1	49.07	2.34	14.61	11.19	0.11	7.25	9.15	2.92	1.46	0.58	0.97	99.64	60.2
GS4–1	48.33	2.10	13.34	10.53	0.15	8.91	9.58	2.67	1.48	0.51	2.27	99.87	66.4
GS5–1	49.30	2.17	13.50	10.69	0.13	7.31	9.11	2.93	1.59	0.51	1.84	99.06	61.4
GS5–2	50.04	2.34	14.67	10.69	0.10	5.26	9.10	3.32	1.73	0.57	1.55	99.37	53.4
GS6–1	49.30	2.31	13.88	11.08	0.13	7.11	9.57	2.63	1.66	0.58	1.38	99.64	59.9
GS6–2	48.21	2.57	15.29	11.89	0.11	6.04	7.97	2.47	1.71	0.64	2.85	99.77	54.2
WZ-1	48.94	2.26	13.98	10.28	0.14	7.04	9.77	3.00	1.80	0.55	1.70	99.45	61.5

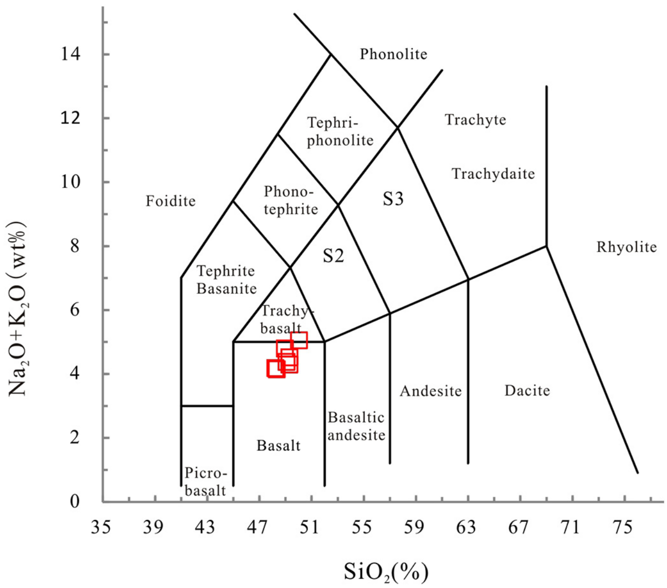

Fig. 2. Total alkali–silica diagram for the Weizhou Island basalts.

pyroxene, and olivine. Plagioclase crystals are euhedral–subhedral and display polysynthetic twinning. Pyroxene and minor olivine form the matrix between plagioclase crystals.

3. Analytical methods

Whole-rock major element analyses were conducted by X-ray fluorescence (XRF) (Primus II, Rigaku, Japan) at Wuhan Sample Solution Analytical Technology Co., Ltd., Wuhan, China. Chemical analysis methods for silicate rocks followed Chinese National Standard GB/T 14506.28-2010 were used to determine the contents of 16 major elements. The analytical precision of major-element contents is better than 5%.

Whole-rock trace-element analyses were conducted using an Agilent 7700e inductively coupled plasma–mass spectrometer (ICP–MS) at Wuhan Sample Solution Analytical Technology. Sample preparation and analytical procedures followed those described by Liu et al. (2008). The analytical precision of trace-element contents is better than 5%.

Whole-rock Sr–Nd–Pb–Hf isotope data were measured on a Neptune Plus multicollector–ICP–MS instrument at Wuhan Sample Solution Analytical Technology. Mass discrimination correction was carried out via internal normalization using an $^{88}Sr/^{86}Sr$ ratio of 8.375209 and a $^{146}Nd/^{144}Nd$ ratio of 0.7219 (Lin et al., 2016). NIST SRM-987 and JNdi-1 were used as certified reference standard solutions for $^{87/86}Sr$ and $^{143/144}Nd$ isotope ratios, with results of $^{87}Sr/^{86}Sr = 0.710244 \pm 22$ ($n = 32$) and $^{143}Nd/^{144}Nd = 0.512118 \pm 15$ ($n = 31$). In addition, USGS reference materials BCR-2 (basalt) and RGM-2 (rhyolite) yielded results of 0.705034 ± 0.000014 (2σ, $n = 4$) and 0.704192 ± 0.000010 (2σ, $n = 4$) for $^{87}Sr/^{86}Sr$, and 0.512644 ± 0.000015 (2σ, $n = 6$) and 0.512810 ± 0.000015 (2σ, $n = 4$) for $^{143}Nd/^{144}Nd$, respectively, which are within error of their published values (Li et al., 2012).

All measured Pb isotope ratios were normalized to the established NBS SRM 981 values of $^{208}Pb/^{204}Pb = 36.7262 \pm 0.0003$, $^{207}Pb/^{204}Pb = 15.5000 \pm 0.0013$, and $^{206}Pb/^{204}Pb = 16.9416 \pm 0.0013$ (Baker et al., 2004). In addition, USGS reference material BCR-2 (basalt) yielded $^{208}Pb/^{204}Pb = 38.743 \pm 0.017$, $^{207}Pb/^{204}Pb = 15.624 \pm 0.003$, and $^{206}Pb/^{204}Pb = 18.763 \pm 0.008$ (2SD, $n = 4$), which are within 0.03% of their published values (Baker et al., 2004).

The analyzed $^{176}Hf/^{177}Hf$ ratios were normalized to $^{179}Hf/^{177}Hf = 0.7325$ (Lin et al., 2016). Analyses of the JMC 475 standard yielded a

Table 2
Trace-element compositions for Quaternary basalts from Weizhou Island, northwestern South China Sea.

	GS2-1	GS4-1	GS5-1	GS5-2	GS6-1	GS6-2	WZ-1
Li	10.8	7.57	9.75	10.0	8.13	11.5	9.60
Be	1.43	1.35	1.42	1.42	1.43	1.07	1.55
Sc	19.3	17.8	20.5	20.0	20.3	22.3	18.8
V	175	170	182	180	188	194	192
Cr	289	281	334	308	318	396	257
Co	47.2	45.1	44.5	48.1	45.8	51.4	41.6
Ni	189	173	181	156	190	197	119
Cu	53.6	51.3	48.3	60.4	47.6	53.4	47.4
Zn	108	103	105	116	120	140	101
Ga	22.1	20.0	20.1	22.0	21.5	22.7	20.7
Rb	20.0	27.0	29.1	26.6	29.4	24.3	33.4
Sr	806	633	615	749	727	569	752
Y	23.7	18.1	21.0	31.4	22.1	22.4	18.1
Zr	182	157	158	175	180	192	177
Nb	53.1	44.3	45.9	50.3	53.1	56.3	50.7
Sn	1.55	1.46	1.45	1.64	1.64	1.73	1.70
Cs	0.19	0.42	0.55	0.34	0.18	0.15	0.61
Ba	442	378	393	446	514	554	428
La	34.4	26.1	27.3	36.7	33.9	36.8	30.2
Ce	61.8	51.5	52.9	58.5	61.6	63.4	57.7
Pr	7.28	5.97	6.37	7.43	7.48	8.03	6.91
Nd	31.3	25.6	27.8	31.9	31.4	32.9	28.5
Sm	6.64	5.68	6.07	7.11	7.00	7.26	6.06
Eu	2.24	1.87	1.98	2.28	2.26	2.51	2.24
Gd	6.73	5.24	6.11	7.08	6.80	7.09	5.61
Tb	0.95	0.75	0.85	0.99	0.96	1.03	0.81
Dy	4.68	3.89	4.14	4.95	4.69	4.79	4.06
Ho	0.83	0.69	0.76	0.94	0.81	0.90	0.73
Er	2.06	1.56	1.99	2.29	2.05	2.00	1.75
Tm	0.22	0.19	0.22	0.26	0.24	0.23	0.22
Yb	1.44	1.23	1.29	1.48	1.44	1.37	1.33
Lu	0.20	0.16	0.18	0.23	0.19	0.20	0.16
Hf	4.28	3.67	3.92	4.22	4.34	4.64	4.22
Ta	2.76	2.36	2.52	2.74	2.85	3.06	2.74
Tl	0.020	0.017	0.021	0.026	0.026	0.015	0.038
Pb	2.75	2.40	2.30	2.97	2.80	2.75	2.63
Th	4.31	3.68	3.83	4.27	4.57	4.86	4.05
U	0.85	0.91	0.73	0.72	0.55	0.70	1.24
ΣREE	160.78	130.45	138.00	162.06	160.78	168.54	146.31
LREE	143.67	116.73	122.46	143.83	143.61	150.93	131.64
HREE	17.11	13.72	15.55	18.23	17.18	17.60	14.67
LREE/HREE	8.40	8.51	7.88	7.89	8.36	8.57	8.97
La_N/Yb_N	17.06	15.23	15.19	17.76	16.92	19.29	16.30
δEu	1.03	1.05	1.00	0.98	1.00	1.07	1.17

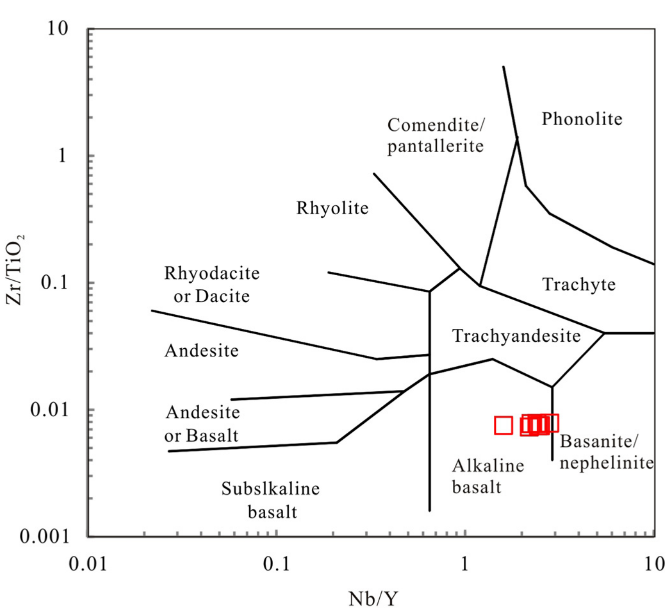

Fig. 3. Geochemical Zr/TiO_2 vs. Nb/Y classification diagram for the Weizhou Island basalts (Winchester and Floyd, 1977).

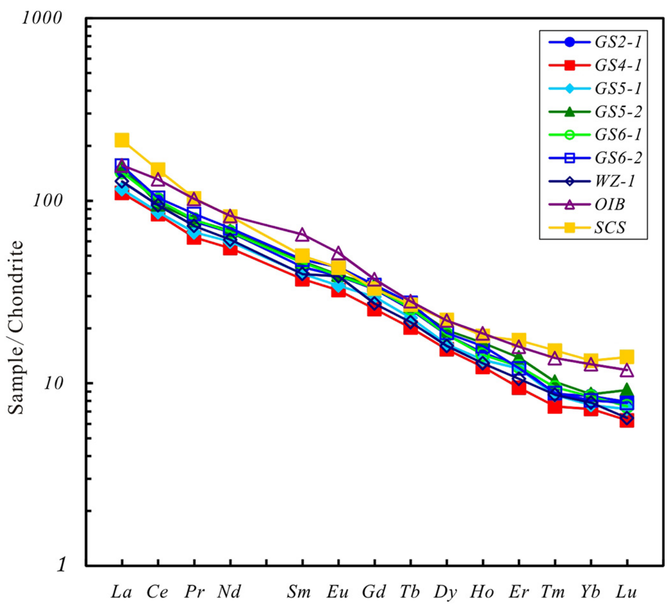

Fig. 4. Chondrite-normalized REE patterns for the Weizhou Island basalts. Data for chondrites and OIBs are from Sun and McDonough (1989); data for the SCS are from Yan et al. (2008).

^{176}Hf /^{177}Hf ratio of 0.212861 ± 0.000013 (2SD, $n = 12$), which is within error of the published value (0.282163 ± 0.000021; Weis et al., 2007). In addition, analyses of the USGS reference material BCR-2 (basalt) yielded a value of 0.282865 ± 0.000010 (2SD, $n = 4$) for ^{176}Hf /^{177}Hf, which is within error of the published value (Weis et al., 2007).

4. Results

Major-element compositions of the studied Weizhou Island basalt samples are given in Table 1. All of the analyzed samples exhibit narrow compositional ranges. SiO_2 contents range from 48.21 to 50.04 wt%, TiO_2 from 2.1 to 2.57 wt%, Al_2O_3 from 13.34 to 15.29 wt%, $^{T}Fe_2O_3$ from 10.28 to 11.89 wt%, MgO from 5.26 to 8.91 wt%, Na_2O from 2.63 to 3.32 wt%, K_2O from 1.46 to 1.8 wt%, and Mg# from 53.4 to 66.4. In a total alkali–silica (TAS) diagram (Fig. 2), all of the samples plot in the basalt field. In a Zr/TiO_2 vs. Nb/Y diagram (Winchester and Floyd, 1977) (Fig. 3), all of the analyzed samples fall in the field of alkaline basalt.

Trace-element and REE compositions of the analyzed basalt samples are given in Table 2. Total REE contents (ΣREEs) of the samples vary from 130.45 to 168.54 ppm, with a mean of 152.42 ppm, which is slightly lower than the average OIB value (198.9 ppm; Sun and McDonough, 1989). In a chondrite-normalized REE diagram (Fig. 4), the basalt samples exhibit enrichment in light REEs (LREEs), with $(La/Yb)_N$ values of 15.19–19.29 (mean of 16.82). Eu/Eu* values of the samples range from 0.98 to 1.17 (mean of 1.04). The lack of negative Eu anomalies in the basalts may reflect a high Eu^{+3}/Eu^{+2} ratio in the magmas (Frey et al., 1993). REE patterns are similar to those of the SCS and intra-plate OIBs (Sun and McDonough, 1989; Yan et al., 2008).

In a primitive-mantle-normalized trace-element spider diagram (Fig. 5), the studied basalts display similar distribution patterns to those of basalts from the SCS. The analyzed samples are characterized by enrichment in large-ion lithophile elements (LILEs) (e.g., Ba) and high-field-strength elements (HFSEs) (e.g., Nb and Ta), and negative U and Yb anomalies. Overall, the trace-element patterns of the basalts are similar to those of intraplate OIBs (Sun and McDonough, 1989; Yan et al., 2008).

The Weizhou Island basalts have relatively homogeneous whole-rock Hf–Sr–Nd–Pb isotope compositions (Table 3). Hf–Sr–Nd–Pb isotope compositions for the samples are as follows: $^{176}Hf/^{177}Hf$ = 0.283012–0.283032, $^{87}Sr/^{86}Sr$ = 0.703591–0.703703, $^{143}Nd/^{144}Nd$ = 0.512897–0.512931, $^{206}Pb/^{204}Pb$ = 18.6117–18.7505, $^{207}Pb/^{204}Pb$ = 15.5953–15.6528, and $^{208}Pb/^{204}Pb$ = 38.7292–38.9109. In $^{207}Pb/^{204}Pb$ vs. $^{206}Pb/^{204}Pb$ and $^{208}Pb/^{204}Pb$ vs. $^{206}Pb/^{204}Pb$ diagrams (Fig. 6), all of the Cenozoic basalts lie above the Northern Hemisphere reference line (NHRL), similar to the Dupal anomaly in the Southern Hemisphere (Hart, 1984; Tu et al., 1991; Flower et al., 1992).

5. Discussion

5.1. Petrogenesis

5.1.1. Crustal contamination and fractional crystallization

The composition of basaltic magmas can be modified by crustal contamination during ascent through the continental crust to the surface (Dai et al., 2018; Wang et al., 2019; Xu et al., 2005; Zeng et al., 2013). Thus, the effects of crustal contamination need to be evaluated before

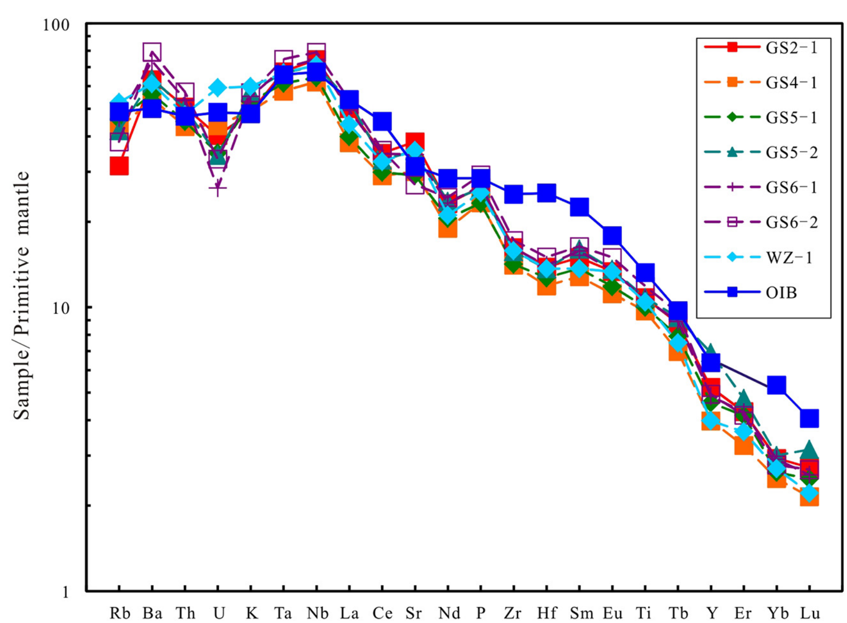

Fig. 5. Primitive-mantle-normalized trace-element diagram for the Weizhou Island basalts. Data for the primitive mantle and OIB are from Sun and McDonough (1989).

Table 3
Hf–Sr–Nd–Pb isotope ratios for Quaternary basalts from Weizhou Island, northwestern South China Sea.

	$^{87}Sr/^{86}Sr$	2σ	$^{143}Nd/^{144}Nd$	2σ	$^{206}Pb/^{204}Pb$	2σ	$^{207}Pb/^{204}Pb$	2σ	$^{208}Pb/^{204}Pb$	2σ	$^{176}Hf/^{177}Hf$	2σ
GS2-1	0.703591	0.000008	0.51291	0.000008	18.6415	0.0008	15.6015	0.0007	38.7575	0.0018	0.283032	0.000004
GS4-1	0.703610	0.000010	0.512902	0.000010	18.6614	0.0008	15.6082	0.0007	38.7903	0.0019	0.283025	0.000006
GS5-1	0.703656	0.000009	0.512919	0.000010	18.6117	0.0010	15.6079	0.0009	38.7292	0.0023	0.283021	0.000007
GS5-2	0.703665	0.000008	0.512915	0.000009	18.6836	0.0009	15.6179	0.0008	38.8298	0.0019	0.283022	0.000005
GS6-1	0.703620	0.000009	0.512931	0.000010	18.6384	0.0009	15.5953	0.0008	38.7523	0.0022	0.283021	0.000007
GS6-2	0.703680	0.000007	0.512925	0.000010	18.6526	0.0008	15.5998	0.0007	38.7721	0.0018	0.283029	0.000005
WZ-1	0.703703	0.000007	0.512897	0.000011	18.7505	0.0006	15.6528	0.0005	38.9109	0.0012	0.283012	0.000009

deciphering the nature of the mantle source for the Weizhou Island Quaternary basalts. Previous studies have proposed that crustal contamination can be identified from trace-element and isotopic data (An et al., 2017; Dai et al., 2018; Rudnick and Gao, 2003; Salters and Stracke, 2004). The Weizhou Island basalts have relatively variable Nb/U (40.81–96.36, mean of 65.99) and Ce/Pb (19.67–23.03) ratios that are substantially higher than those of continental crust (Nb/U = 6.15 and Ce/Pb = 3.91; Rudnick and Gao, 2003; Salters and Stracke, 2004), suggesting limited crustal contamination. Furthermore, the absence of obvious Zr or Hf anomalies in the studied basalts rules out significant crustal contamination because Zr and Hf are generally enriched in crustal materials (Rudnick and Gao, 2003; Wang et al., 2019; Zhao et al., 2010). Moreover, a trace-element spider diagram (Fig. 5) lacks strong negative Nb or Ta anomalies, which further supports negligible continental crustal contamination (Zou et al., 2003; Yang et al. 2015; An et al., 2017). In conclusion, crustal contamination of the Weizhou Island basalts is negligible, and these rocks were therefore likely derived from mantle sources.

Fractional crystallization can play an important role in the evolution of a magma. The Weizhou Island basalts have Mg# values of 53.4–66.4, Cr contents of 257–396 ppm, and Ni contents of 119–197 ppm, much lower than the values for primitive basalts (Mg# > 70, Cr > 1000 ppm, and Ni > 400 ppm) (An et al., 2017; Wang et al., 2019; Wilkinson and Le Maitre, 1987), indicating that these basalts have experienced fractional crystallization. The SiO_2, $Fe_2O_3^T$, Al_2O_3, and K_2O contents of the analyzed samples show a negative relationship with Mg# values, whereas CaO and CaO/Al_2O_3 ratios show a positive relationship (Fig. 7), together indicating that the formation of these basalts involved the fractionation of olivine and clinopyroxene.

5.1.2. Mantle source characteristics

As established above, the Weizhou Island basalts were not substantially affected by crustal contamination. As fractional crystallization does not change the isotope ratios of magma, the isotope ratios of the analyzed samples can be used to explore the mantle source beneath the study area. The Hf–Sr–Nd–Pb isotope compositions for the studied basalts are presented in isotope correlation/discrimination diagrams (Figs. 6 and 8). These diagrams suggest that the basalts can be explained by a binary mixing model involving two mantle end-members (DMM and EM2), which is consistent with Cenozoic basaltic rocks from the SCS and surrounding areas (Jia et al., 2003; Yan et al., 2008, 2015, 2018, 2019; Zou and Fan, 2010; Wang et al., 2012b, 2012c; Huang et al., 2013; Li et al., 2013; Yang and Fang, 2015; An et al., 2017; Zhang et al., 2018b).

The DMM end-member is considered to be Indian MORB-type mantle (An et al., 2017; Hoang et al., 1996, 2013; Yan et al., 2018, 2019). However, the origin of EM2 is uncertain. Previous studies have suggested that EM2 of the SCS is derived from SCLM (Tu et al., 1992a, 1992b; Hoang et al., 1996; Fan et al., 2008; Wang et al., 2012a; Huang et al., 2013; Ren et al., 2013). However, the EM2 in the Weizhou Island basalts may have originated from the Hainan mantle plume rather than from SCLM, as inferred from the following lines of evidence:

(1) Previous research has proposed that the lithosphere beneath the SCS is relatively thin and that the thinning process occurred during the spreading of the SCS; therefore, only small amounts of old SCLM in the SCS remained after the cessation of seafloor spreading (Briais et al., 1993; Wu et al., 2004; Yan et al., 2008; Xu et al., 2012). Thus, we consider that the EM2 component in the Weizhou Island basalts might not have originated from SCLM.

(2) The Weizhou Island basalts exhibit significant positive Nb and Ta

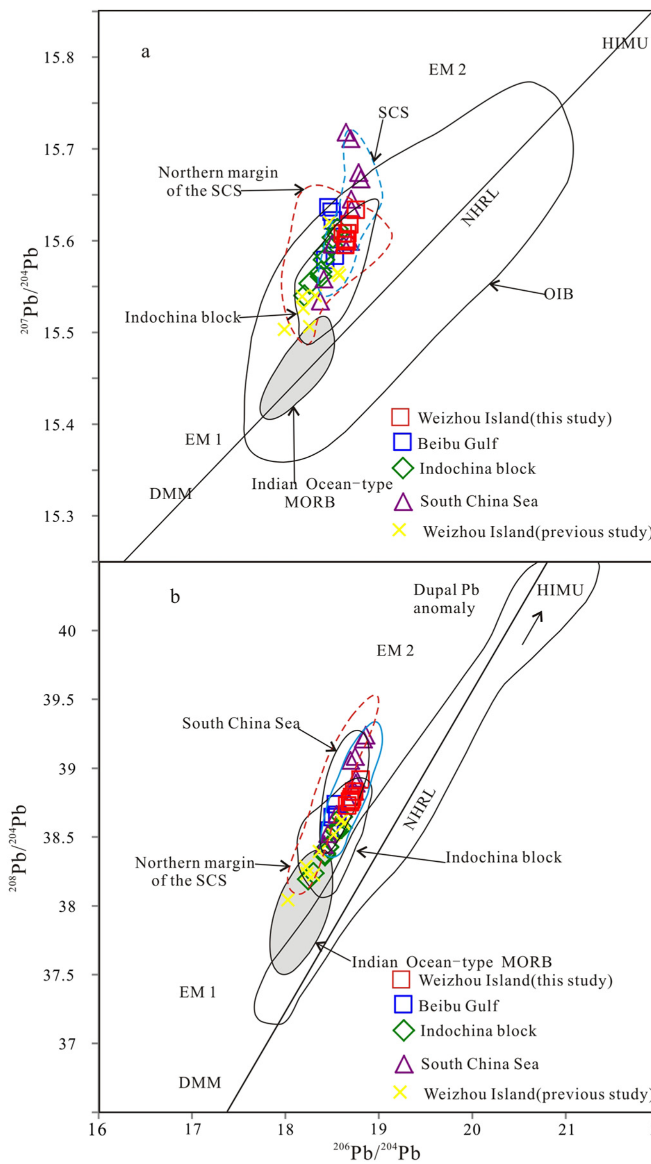

Fig. 6. Plots of (a) $^{207}Pb/^{204}Pb$ vs. $^{206}Pb/^{204}Pb$ and (b) $^{208}Pb/^{204}Pb$ vs. $^{206}Pb/^{204}Pb$ for the studied Weizhou Island basalts. Data for the Beibu Gulf are from Li et al. (2013); data for the Indochina block are from Yan et al. (2018); data for the SCS are from Yan et al. (2008); previous data for Weizhou Island are from Fan et al. (2008). The approximate fields for DMM, HIMU, EM1, EM2, and Indian Ocean-type MORB and OIB are from Salters and White (1998). The Dupal isotopic anomaly is from Hamelin and Allègre (1985). NHRL is the Northern Hemisphere reference line (Hart, 1984).

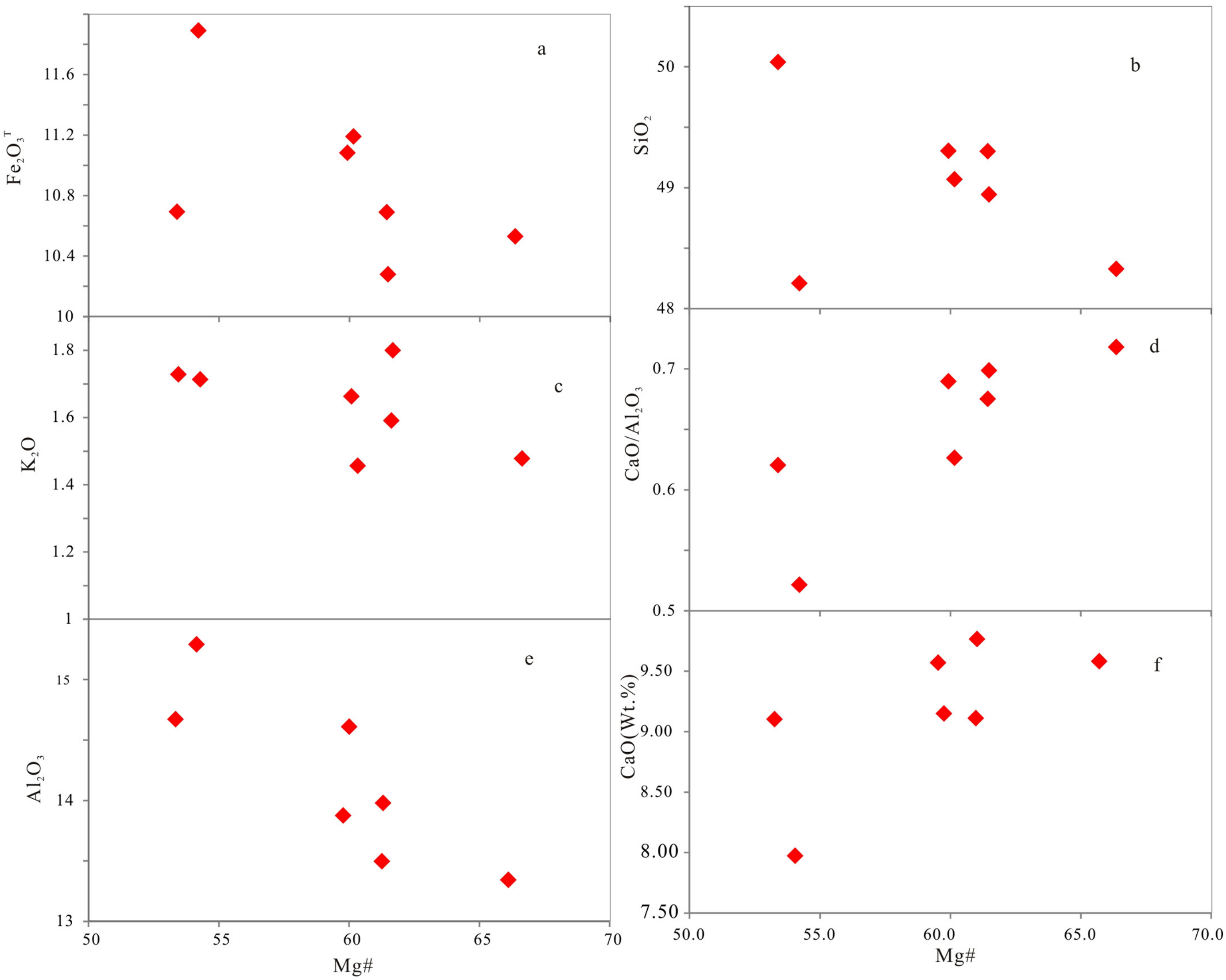

Fig. 7. Variations in selected major-element oxides of Weizhou Island basalts.

anomalies, in contrast to basaltic rocks derived from SCLM (An et al., 2017; Yan et al., 2018; Zou et al., 2003), which also suggests that EM2 did not originate from SCLM.

(3) Yan et al. (2018) reported that SCLM generally shows Hf—Nd isotope compositions that differ from those of oceanic basalts (MORB and OIB). In Fig. 4, all of the analyzed Weizhou Island samples plot in the OIB field, which further excludes the possibility of a contribution from SCLM.

(4) An et al. (2017) reported that the lithospheric mantle is characterized by significant Nd—Hf isotope decoupling (resulting from fluid-driven metasomatism) (Choi and Mukasa, 2012). Nd—Hf isotopes of Quaternary basalts from Weizhou Island and surrounding areas (including the SCS, Vietnam, and Thailand) define a linear array (Fig. 8b), suggesting that EM2 originated from the Hainan mantle plume rather than from SCLM (An et al., 2017; Wang et al., 2012b; Yan et al., 2015, 2018, 2019).

In summary, we suggest that the enriched component for the Weizhou Island basalts probably originated from the Hainan mantle plume, which is consistent with geophysical evidence (Fan et al., 2017; Wei and Chen, 2016; Xia et al., 2016).

5.1.3. The Dupal anomaly on Weizhou Island

The Weizhou Island basalts exhibit Dupal-like Pb isotope ratios (Fig. 6). The Dupal isotopic anomaly was first recognized by Dupré and Allègre (1983) in a study of Indian Ocean basalts. Hart (1984) termed this anomaly the “Dupal anomaly” and proposed that it represented abnormal mantle under the oceans of the Southern Hemisphere. The Dupal anomaly is characterized by relatively high $^{208}Pb/^{204}Pb$, $^{207}Pb/^{204}Pb$, and $^{87}Sr/^{86}Sr$ for a given $^{206}Pb/^{204}Pb$ ratio (Hart, 1984; Dupré and Allègre (1983); Zhang et al., 2016b). The Dupal reservoir requires high time-integrated values of Rb/Sr, $^{235}U/Pb$, and Th/U (Hart, 1984). During ocean exploration and investigation programs, multiple Dupal anomalies in the Northern Hemisphere have been observed, including in the SCS and surrounding areas (Yan et al., 2008, 2015; Zou and Fan, 2010; Xu et al., 2012; Zhang et al., 2016a; Xie et al., 2017), indicating that the Dupal anomaly is not specific to a particular region.

There has been considerable debate about the formation mechanism of the Dupal isotopic anomaly in the SCS and surrounding areas (Tu et al., 1991, Tu et al., 1992a, 1992b; Yan et al., 2008, 2015; Zou and Fan, 2010; Xu et al., 2012; Li et al., 2013; Zhang et al., 2016b; Xie et al., 2017). Because southeastern China may once have been a part of Gondwana, some scholars have proposed that the Dupal anomaly in the SCS

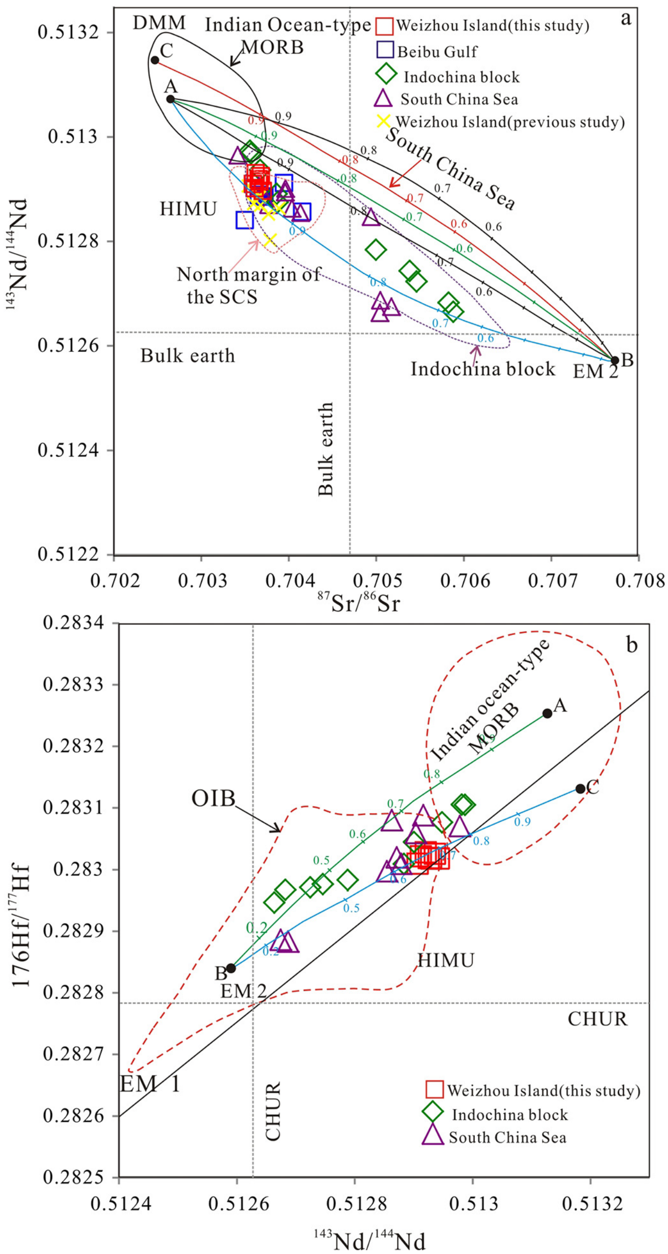

Fig. 8. $^{143}Nd/^{144}Nd$ vs. $^{87}Sr/^{86}Sr$ and $^{176}Hf/^{177}Hf$ vs. $^{143}Nd/^{144}Nd$ plots for the Weizhou Island basalts. Data sources are as in Fig. 6.

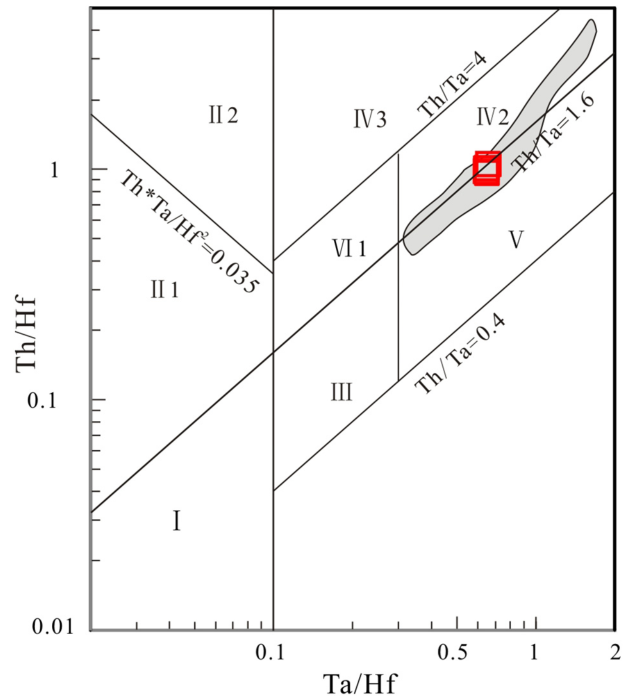

Fig. 9. Discrimination diagrams of Th/Hf vs. Ta/Hf for Weizhou Island basalts (Wang et al., 2001). I: N-MORB from divergent margins; II-1: oceanic island-arc basalt; II-2: continental-margin island-arc and volcanic-arc basalt; III: oceanic intraplate island and seamount basalt, T-MORB, and *E*-MORB; IV-1: tholeiite in intracontinental and continental-margin rifts; IV-2: alkaline basalt in continental rifts; IV-3: basalt in continental extension areas or incipient rifts; V: mantle-plume basalt. Data for the SCS are from Yan et al. (2008).

and surrounding areas may be related to the breakup of Gondwana (Tu et al., 1991, Tu et al., 1992a, 1992b; Zou et al., 2000). However, plate tectonic processes, including those related to the disintegration of a supercontinent, are generally limited to lithospheric levels and do not cause substantial movement of the asthenospheric mantle (Yan et al., 2008; Xu et al., 2012). Furthermore, Cenozoic basalts in the North China Craton show evidence of a Dupal anomaly (Xu et al., 2018; Yan et al., 2007; Zou et al., 2010), which further suggests that the Dupal anomaly in the SCS and surrounding areas was not derived from the Southern Hemisphere.

The most recent research results show that the Dupal anomaly in the SCS and surrounding areas was formed by in situ processes as an endogenetic anomaly and that its formation was closely related to the Hainan mantle plume (Yan et al., 2008, 2015; Zou and Fan, 2010; Shi and Yan, 2011; Xu et al., 2012; Li et al., 2013; Zhang et al., 2016a, 2016b; Zhang et al., 2018b). On the basis of the above discussion, we suggest that the Dupal anomaly on Weizhou Island is related to the Hainan mantle plume (for a discussion on the Hainan mantle plume, see Section 5.2).

5.2. Tectonic significance

Generally, mantle-plume-derived basalts show OIB characteristics, although magma with such characteristics is not necessarily the product of a mantle plume (Niu, 2009; Xu et al., 2012; Wang et al., 2019). In a (Th/Hf)–(Th/Ta) discrimination diagram (Fig. 9d) (Wang et al., 2001), the Weizhou Island basalts plot in the field of plume-derived basalts, consistent with features of basaltic rocks from the SCS and surrounding areas (An et al., 2017; Li et al., 2013; Yan et al., 2008, 2018, 2019). Thus, we conclude that the Weizhou Island basalts likely formed in a mantle plume setting.

The existence of the Hainan mantle plume has been verified by numerous geophysical investigations (Lebedev and Nolet, 2003; Huang, 2014; Wei and Chen, 2016; Xia et al., 2016; Fan et al., 2017). The presence of a mantle plume beneath Vietnam was first proposed by Maruyama (1994). Using seismic tomography, a near-vertical cylindrical low-velocity zone has been observed beneath Hainan Island and the SCS, indicating a possible mantle plume beneath Hainan Island (Lebedev and Nolet, 2003;Huang, 2014; Huang et al., 2015). Several geophysical studies have further proposed that the Hainan mantle plume is one of 12 plumes that originated from the core–mantle boundary (Huang, 2014; Huang et al., 2015). The existence of the Hainan mantle plume has been supported by petrological and geochemical data from the SCS and surrounding areas (Wang et al., 2012b, 2013; Xu et al., 2012; Li et al., 2013; Yan et al., 2014, 2015, 2018, 2019; An et al., 2017; Liu et al., 2017; Zhang et al., 2018b). The Hainan mantle plume may be more complex than other plumes (e.g., the Hawaiian plume) because of the influence of deep subduction (Wang et al., 2013).

Seismic evidence suggests that the bulk part of the Hainan mantle plume is located beneath the Leizhou Peninsula and has a diameter of

~160 km at the depth of the Moho (Wei and Chen, 2016). Xia et al. (2016) proposed that the Hainan mantle plume rises subvertically from the lower mantle beneath South China. The magma accumulates in the mantle transition zone, diffuses laterally, and then ascends further and forms multiple branches. Where rising material reaches the base of the lithosphere, a pancake-shaped anomaly is formed, and this feeds the Hainan hotspot. Based on the above discussions, we suggest that Quaternary basalts from Weizhou Island may be genetically related to the Hainan mantle plume, as are Quaternary basalts in the Beibu Gulf (Li et al., 2013).

Fan et al. (2017) performed numerical simulations of intraplate seamounts in the northern SCS, treating the seamounts as elliptical cones. Those authors calculated that the total volume of magma erupted above the seafloor is between 1885 and 3078 km^3 and that the total amount of intrusive magma above the Moho is ~150,000 km^3, similar to the average value for large igneous provinces (LIPs) worldwide. Furthermore, the area covered by seamounts in the northern SCS is 150,000 km^2, which exceeds the average value for LIPs (Xia et al., 2012; Chen and Xu, 2017; Ernst and Ernst and Youbi, 2017).

Extensive Cenozoic intraplate volcanism has occurred in the SCS and surrounding areas, including the Leiqiong Peninsula, the Beibu Gulf, the PRMB, and the Indochina block. Geochemical studies have shown that these Cenozoic volcanic rocks are composed mainly of OIB-type basalts related to the Hainan mantle plume (An et al., 2017; Wang et al., 2013; Xia et al., 2016; Yan et al., 2014, 2015, 2018, 2019). The Hainan mantle plume has been active from the early Cenozoic to the present (Yan and Shi, 2007; Shi and Yan, 2011). The Pleistocene OIB-type basalts on Weizhou Island suggest that the Hainan mantle plume remains active.

On the basis of the above discussion, we propose the existence of a Cenozoic LIP in the SCS, and surrounding areas and that this LIP is related to the Hainan mantle plume. The plume may have triggered the opening of the SCS (Shi and Yan, 2011; Yan et al., 2018, 2019; Zhang et al., 2018b).

6. Conclusions

This study presents new whole-rock major- and trace-element and Hf–Sr–Nd–Pb isotope data for Quaternary basalts from Weizhou Island in the northwestern SCS. The basalts belong to the alkaline magma series and are characterized by OIB-like geochemical features with enrichments in LREEs, LILEs, and HFSEs. Radiogenic isotope compositions show that the Weizhou Island basalts can be explained by a binary mixing model involving two mantle end-members: DMM and EM2. The EM2 end-member was probably derived from the Hainan mantle plume. A large Cenozoic igneous province likely exists in the SCS and surrounding areas and may be related to the Hainan mantle plume.

Declaration of Competing Interest

The authors declare no conflict of interest.

Acknowledgments

This work was funded by the Natural Science Foundation of China (Grant No. 91428203), the Guangxi scientific projects (Nos. AD17129063 and AA17204074), the Bagui Scholarship of Guangxi Province, Guangxi Youth Science Fund Project (2019GXNSFBA185016), the Ph.D. Research Start-up Foundation of Guangxi University (XBZ170339), and the Basic Ability Improvement Project for Young-Middle Teachers (2018KY0045). We are grateful to two anonymous reviewers who provided constructive suggestions regarding an earlier version of the paper. We thank editor Xianhua Li for his critical review and advice.

References

An, A., Choi, S., Yu, Y., Lee, D., 2017. Petrogenesis of late Cenozoic basaltic rocks from southern Vietnam. Lithos 272–273, 192–204.
Baker, J., Peate, D., Waight, T., Meyzen, C., 2004. Pb isotopic analysis of standards and samples using a ^{207}Pb-^{204}Pb double spike and thallium to correct for mass bias with a double-focusing MC-ICP-MS. Chem. Geol. 211 (3–4), 275–303.
Briais, A., Patriat, P., Tapponier, P., 1993. Updated interpretation of magnetic anomalies and seafloor spreading stages in the South China Sea: implications for the Tertiary tectonics of Southeast Asia. Journal of Geophysical Research 98 (B4), 6299–6328.
Chen, J., Xu, Y.G., 2017. Permian large Igneous Provinces and their Impact on Paleoenvironment and Biodiversity: Progresses and Perspectives. Bull. Mineral. Petrol. Geochem. 36 (3), 374–393 (in Chinese with English abstract).
Choi, S.H., Mukasa, S.B., 2012. Lu-Hf and Sm-Nd isotope systematics of Korean spinel peridotites: a case for metasomatically induced Nd-Hf decoupling. Lithos 154, 263–276.
Dai, L.Q., Zheng, F., Zhao, A.F., Zheng, Y.F., 2018. Geochemical insights into the lithology of mantle sources for Cenozoic alkali basalts in West Qinling, China. Lithos 302-303, 86–98.
Dupré, B., Allègre, C.J., 1983. Pb-Sr isotope variation in Indian Ocean basalts and mixing phenomena. Nature 303, 142–146.
Ernst, R.E., Youbi, N., 2017. How large Igneous Provinces affect global climate, sometimes cause mass extinctions, and represent natural markers in the geological record. Palaeogeogr. Palaeoclimatol. Palaeoecol. 478, 30–52.
Fan, Q.C., Sun, Q., Long, A.M., Sui, J.L., Li, N., Wang, T.H., 2006. Geology and eruption history of volcanoes in Weizhou Island and Xieyang Island, Northern Bay. Acta Petrol. Sin. 22 (6), 1529–1537 in Chinese with English abstract.
Fan, Q.C., Sun, Q., Sui, J.L., Li, N., 2008. Trace-element and isotopic geochemistry of volcanic rocks and its tectonic implications in Weizhou Island and Xieyang Island, Northern Bay (in Chinese). Acta Petrol. Sin. 24 (6), 1323–1332 in Chinese with English abstract.
Fan, C.Y., Xia, S.H., Zhao, F., Sun, J.L., Cao, J.H., Xu, H.L., Wan, K.Y., 2017. New insights into the magmatism in the northern margin of the South China Sea: spatial features and volume of intraplate seamounts. Geochem. Geophys. Geosyst. 18 (6), 2216–2239.
Flower, M.F.J., Zhang, M., Chen, C.Y., Tu, K., Xie, G.H., 1992. Magmatism in the South China Basin 2. Post-spreading Quaternary basalts from Hainan Island, south China. Chemical Geology 97, 65–87.
Frey, F.A., Garcia, M.O., Wise, W.S., Kennedy, A., Gurriet, P., Albarede, F., 1993. The evolution of Mauna Kea volcano, Hawaii: petrogenesis of tholeiitic and alkali basalts. J. Geophys. Res. 96, 14347–14375.
Gao, J.W., Wu, S.G., McIntosh, K., Mi, L.J., Yao, B.C., Chen, Z.M., Jia, L.K., 2015. The continent–ocean transition at the mid-northern margin of the South China Sea. Tectonophysics 654, 1–19.
Hamelin, B., Allègre, C.J., 1985. Large scale regional units in the depleted upper mantle revealed by an isotopic study of the south-west Indian ridge. Nature 315, 196–198.
Hart, S.R., 1984. A large-scale isotope anomaly in the Southern Hemisphere mantle. Nature 309, 753–757.
Hoang, N., Flower, M., Carlson, R.W., 1996. Major, trace element, and isotopic compositions of Vietnamese basalts: interaction of hydrous EM1-rich asthenosphere with thinned Eurasian lithosphere. Geochim. Cosmochim. Acta 60 (22), 4329–4351.
Hoang, N., Flower, M.F.J., Chi, C.T., Xuan, P.T., Quy, H.V., Son, T.T., 2013. Collisioninduced basalt eruptions at Pleiku and Buon Me Thuot, south-central Viet Nam. J. Geodyn. 69, 65–83.
Huang, J., 2014. P-and S-wave tomography of the Hainan and surrounding regions: insight into the Hainan plume. Tectonophysics 633, 176–192.
Huang, L.P., Li, C.N., 2007. Peridotite xenolith fragments from Late Quaternary pyroclastic flow in Weizhou Island, Beihai, Guangxi. Acta Petrol. Mineral. 26 (4), 321–328 in Chinese with English abstract.
Huang, X.L., Niu, Y.L., Xu, Y.G., Ma, J.L., Qiu, H.N., Zhong, J.W., 2013. Geochronology and geochemistry of Cenozoic basalts from eastern Guangdong, SE China: constraints on the lithosphere evolution beneath the northern margin of the South China Sea. Contributions to Mineralogy & Petrology 165 (3), 437–455.
Huang, Z.C., Zhao, D.P., Wang, L.S., 2015. P wave tomography and anisotropy beneath Southeas Asia: insight into mantle dynamics. J. Geophys. Res. Solid Earth 120, 5154–5174.
Jia, D.C., Qiu, X.L., Hu, R.Z., Lu, Y., 2003. Geochemical nature of mantle reservoirs and tectonic setting of basalts in Beibu Gulf and its adjacent region. J. Trop. Ocean. 22 (2), 30–39 in Chinese with English abstract.
Lebedev, S., Nolet, G., 2003. Upper mantle beneath southeast Asia from S velocity tomography. J Geophys Res 108, 20–48.
Li, N., Fan, Q.C., Wang, T.H., Sun, Q., Sui, J.L., 2006. Preliminary study on K-Ar chronology, petrology and geochemistry of Yandunling volcanic rocks, Hepu county, Guangxi. Acta Petrol. Sin. 23 (6), 1423–1430 (in Chinese with English abstract).
Li, C.F., Li, X.H., Li, Q.L., Guo, J.H., Yang, Y.H., 2012. Rapid and precise determination of Sr and Nd isotopic ratios in geological samples from the same filament loading by thermal ionization mass spectrometry employing a single-step separation scheme. Anal. Chim. Acta 727 (10), 54–60.
Li, N.S., Yan, Q.S., Chen, Z.H., Shi, X.F., 2013. Geochemistry and petrogenesis of Quaternary volcanism from the islets in the eastern Beibu Gulf: evidence for Hainan plume. Acta Ocean. Sinica, 2013 32 (12), 40–49.
Li, C.F., Xu, X., Lin, J., Sun, Z., Zhu, J., Yao, Y.J., Zhao, X.X., Liu, Q.S., Kulhanek, D.K., Wang, J., Song, T., Zhao, J.F., Qiu, N., Guan, Y.X., Williams, T., Bao, R., Briais, A., Brown, E.A., Chen, Y.F., Clift, P.D., Colwell, F.S., Dadd, K.A., Ding, W.W., Almeida, I.H., Huang, X.L., Hyun, S.M., Jiang, T., Koppers, A.A.P., Li, Q.Y., Liu, C.L., Liu, Z.F., Nagai, R.H., Peleo-Alampay, A., Su, X., Tejada, M.L.G., Trinh, H.S., Yeh, Y.C., Zhang, C.L., Zhang, F., Zhang, G.L., 2014. Ages and magnetic structures of the South China Sea constrained by deep tow magnetic surveys and IODP Expedition 349. Geochem. Geophys. Geosyst. 15 (12), 4958–4983.

Lin, J., Liu, Y.S., Yang, Y.H., Hu, Z.C., 2016. Calibration and correction of LA-ICP-MS and LA-MC-ICP-MS analyses for element contents and isotopic ratios. Solid Earth Sci. 1, 5–27.

Liu, Y.S., Zong, K.Q., Kelemen, P.B., Gao, S., 2008. Geochemistry and magmatic history of eclogites and ultramafc rocks from the Chinese continental scientifc drill hole: subduction and ultrahigh-pressure metamorphism of lower crustal cumulates. Chem. Geol. 247, 133–153.

Liu, E.T., Wang, H., Uysal, T., Zhao, J.X., Wang, X.C., Feng, Y.X., Pan, S.Q., 2017. Paleogene igneous intrusion and its effect on thermal maturity of organic-rich mudstones in the Beibuwan Basin, South China Sea. Mar. Pet. Geol. 86, 733–750.

Maruyama, S., 1994. Plume tectonics. J. Geol. Soc. Jpn. 100, 24–29.

Sun, S.S., McDonough, W.F., 1989. Chemical and isotopic systemtics of oceanic basalts: Implications of mantle composition and processes. Geol. Soc. Lond. Spec. Publ. 42, 313–345.

Niu, Y.L., 2009. Some basic concepts and problems on the petrogenesis of intra-plate Ocean island basalts. Chin. Sci. Bull. 54, 4148–4160.

Ren, J.B., Wang, L.L., Yan, Q.S., Shi, X.F., Liao, L., Fang, N.Q., 2013. Geochemical characteristics and its geological implications for basalts in volcanicalstic rock from Daimao seamount. Earth Sci. J. China Uni. Geosci. 38 (S1), 10–20 in Chinese with English abstract.

Rudnick, R.L., Gao, S., 2003. Composition of the continental crust. Treatise Geochem. 3, 1–64.

Salters, V.J.M., Stracke, A., 2004. Composition of the depleted mantle. Geochem. Geophys. Geosyst. 15 (5), Q05004.

Salters, V.J.M., White, W.M., 1998. Hf isotope constraints on mantle evolution. Chem. Geol. 145, 447–460.

Shi, X.F., Yan, Q.S., 2011. Geochemistry of Cenozoic magmatism in the South China Sea and its tectonic implications. Mar. Geol. Quat. Geol. 31 (2), 59–72 in Chinese with English abstract.

Tu, K., Flower, M.F.J., Carlson, R.W., Zhang, M., Xie, G., 1991. Sr, Nd, and Pb isotopic compositions of Hainan basalts (south China): implications for a subcontinental lithosphere Dupal source. Geology 19, 567–569.

Tu, K., Flower, M.F.J., Carlson, R.W., Xie, G.H., Chen, C.Y., Zhang, M., 1992a. Magmatism in the South China Basin. Chem. Geol. 97 (1–2), 47–63.

Tu, K., Flower, M.F.J., Zhang, M., Xie, G.H., 1992b. Sr, Nd, and Pb isotopic compositions of Hainan basalts (South China): Implications for a subcontinental lithosphere Dupal source. Geology 19 (6), 325–333.

Wang, Y.L., Zhang, C.J., Xiu, S.Z., 2001. Th/Hf – Ta/Hf identification of tectonic setting of basalts. Acta Petrol. Sin. 17 (3), 413–421 in Chinese with English abstract.

Wang, K.L., Chung, S., Lo, Y.M., Lo, C.H., Yang, H.J., Shinjo, R., Lee, T.Y., Wu, J.C., Huang, S.T., 2012a. Age and geochemical characteristics of Paleogene basalts drilled from western Taiwan: Records of initial rifting at the southeastern Eurasian continental margin. Lithos 155, 426–441.

Wang, X.C., Li, Z.X., Li, X.H., Li, J., Liu, Y., Long, W.G., Zhou, J.B., Wang, F., 2012b. Temperature, pressure, and composition of the mantle source region of late Cenozoic basalts in Hainan Island, SE Asia: a consequence of a young thermal mantle plume close to subduction zones? J. Petrol. 53, 177–233.

Wang, K.L., Lo, Y.M., Chung, S., Lo, C.H., Hsu, S.K., Yang, H.J., Shinjo, R., 2012c. Age and Geochemical Features of Dredged Basalts from Offshore SW Taiwan: the Coincidence of Intra-Plate Magmatism with the Spreading South China Sea. Terr. Atmos. Ocean. Sci. 23 (6), 657–669.

Wang, X.C., Li, Z.X., Li, X.H., Li, J., Xu, Y.G., Li, X.H., 2013. Identification of an ancient mantle reservoir and young recycled materials in the source region of a young mantle plume: Implications for potential linkages between plume and plate tectonics. Earth Planet. Sci. Lett. 377–378, 248–259.

Wang, J., Su, Y.P., Zheng, J.P., Gao, S.L., Dai, H.K., Ping, X.Q., Xiong, Q., Niyw, K., 2019. Geochronology and petrogenesis of Jurassic intraplate alkali basalts in the Junggar terrane, NW China: Implication for low-volume basaltic volcanism. Lithos 324–325, 202–215.

Wei, S.S., Chen, Y.J., 2016. Seismic evidence of the Hainan mantle plume by receiver function analysis in southern China. Geophys. Res. Lett. 43 (17), 8978–8985.

Weis, D., Kieffer, B., Hanano, D., Silva, I.N., Barling, J., Pretorius, W., Maerschalk, C., Mattielli, N., 2007. Hf isotope compositions of U.S. Geological Survey reference materials. Geochem. Geophys. Geosyst. 8 (6), Q06006 2007.

Wilkinson, J.F.G., Le Maitre, R.W., 1987. Upper mantle amphiboles and micas and TiO_2, K_2O, and P_2O_5 abundances and 100 $Mg/(Mg + Fe^{2+})$ ratios of common basalts andandesites: implications for modal mantle metasomatism and undepleted mantle compositions. J. Petrol. 28, 37–73.

Winchester, J.A., Floyd, P.A., 1977. Geochemical discrimination of different magma series and their differentiation products using immobile elements. Chem. Geol. 20, 325–343.

Wu, H.H., Tsai, Y.B., Lee, T.Y., Lo, C.H., Hsieh, C.H., Toan, D.V., 2004. 3-D shear wave velocity structure of the crust and upper mantle in South China Sea and its surrounding regions by surface wave dispersion analysis. Mar. Geophys. Res. 2004 (25), 5–27.

Xia, L.Q., Xu, X.Y., Li, X.M., Xia, Z.C., Ma, Z.Q., 2012. Comparison of three large igneous provinces (emeishan, siberia, deccan) in Asia. Northwest. Geol. 45 (2), 1–26 in Chinese with English abstract.

Xia, S.H., Zhao, D.P., Sun, J.L., Huang, H.B., 2016. Teleseismic imaging of the mantle beneath southernmost China: New insights into the Hainan plume. Gondwana Res. 36, 46–56.

Xie, A.Y., Zhong, L.F., Yan, W., 2017. Time and genesis of Cenozoic magmatisms in the South China Sea and surrounding areas. Mar. Geol. Quat. Geol. 37 (2), 108–118 in Chinese with English abstract.

Xu, Y.G., Ma, J.L., Frey, F.A., Feigenson, M.D., Liu, J.F., 2005. Role of lithosphere–asthenosphere interaction in the genesis of quaternary alkali and tholeiitic basalts from Datong, western North China craton. Chem. Geol. 224, 247–271.

Xu, Y.G., Wei, J.X., Qiu, H.N., Zhang, H.H., Huang, X.L., 2012. Opening and evolution of the South China Sea constrained by studies on volcanic rocks: Preliminary results and a research design. Chin Sci Bull 57, 3150–3164.

Xu, Y.G., Li, H.Y., Hong, L.B., Ma, L., Ma, Q., Sun, M.D., 2018. Generation of Cenozoic intraplate basalts in the big mantle wedge under eastern Asia. Sci. China Earth Sci. 61, 869–886.

Yan, J., Zhao, J.X., Liu, H.Q., 2007. Quaternary basalts from Longang in the North China Craton: petrogenesis and characteristics of the mantle source. Acta Petrol. Sin. 23 (6), 1413–1422 (in Chinese with English abstract).

Yan, Q.S., Shi, X.F., Wang, K.S., Bu, W.R., Xiao, L., 2008. Major element, trace element, Sr–Nd–Pb isotopic studies of Cenozoic alkali basalts from the South China Sea. Sci. China (Series D) 51 (4), 550–566.

Yan, Q.S., Shi, X.F., Castillo, P., 2014. The late Mesozoic-Cenozoic tectonic evolution of the South China Sea: a petrologic perspective. J. Asian Earth Sci. 85, 178–201.

Yan, Q.S., Castillo, P., Shi, X.F., Wang, L.L., Liao, L., Ren, J.B., 2015. Geochemistry and petrogenesis of volcanic rocks from Daimao Seamount (South China Sea) and their tectonic implications. Lithos 218, 117–126.

Yan, Q.S., Shi, X.F., Metcalfe, F., Liu, S.F., Xu, T.Y., Kornkanitnan, N., Sirichaiseth, T., Yuan, L., Zhang, Y., Zhang, H., 2018. Hainan mantle plume produced late Cenozoic basaltic rocks in Thailand, Southeast Asia. Sci. Rep. 8, 2640.

Yan, Q.S., Straub, S., Shi, X.F., 2019. Hafnium isotopic constraints on the origin of late Miocene to Pliocene seamount basalts from the South China Sea and its tectonic implications. J. Asian Earth Sci. 171, 162–168.

Yang, S.Y., Fang, N.Q., 2015. Geochemical variation of volcanic rocks from the South China Sea and neighboring land: Implication for magmatic process and mantle structure. Acta Oceanol. Sin. 34 (12), 112–124.

Zeng, G., Chen, L.H., Hu, S.L., Xu, X.S., Yang, L.F., 2013. Genesis of Cenozoic low-Ca alkaline basalts in the Nanjing basaltic feld, eastern China: the case for mantle xenolith-magma interaction. Geochem. Geophys. Geosyst. 14, 1660–1677.

Zhang, Q., Wu, S.G., Dong, D.D., 2016a. Cenozoic magmatism in the northern continental margin of the South China Sea: evidence from seismic profiles. Mar. Geophys. Res. 37, 71–94.

Zhang, Z., Li, S.Z., Suo, Y.H., Somerville, I.D., Li, X.Y., 2016b. Formation mechanism of the global Dupal isotope anomaly. Geol. J. 51 (S1), 644–651.

Zhang, Y., Yu, K.F., Qian, H.D., 2018a. LA-ICP-MS analysis of clinopyroxenes in basaltic pyroclastic rocks from the Xisha Islands, Northwestern South China Sea. Minerals 8, 875.

Zhang, G.L., Luo, Q., Zhao, J., Jackson, M.G., Guo, L.S., Zhong, L.F., 2018b. Geochemical nature of sub-ridge mantle and opening dynamics of the South China Sea. Earth Planet. Sci. Lett. 489, 145–155.

Zhang, Y., Yu, K.F., Qian, H.D., Fan, T.L., Yue, Y.F., Wang, R., Jiang, W., Xu, S.D., Wang, Y.H., 2020. The basement and volcanic activities of the Xisha Islands: evidence from the kilometre-scale drilling in the northwestern South China Sea. Geol. J. 55, 571–583.

Zhao, J.H., Zhou, M.F., Zheng, J.P., 2010. Metasomatic mantle source and crustal contamination for the formation of the Neoproterozoic mafic dike swarm in the northern Yangtze Block, South China. Lithos 115, 177–189.

Zhu, B.Q., Wang, H.F., Chen, Y.W., Chang, X.Y., Hu, Y.G., Xie, J., 2002. Geochronological and geochemical constraint on the Cenozoic extension of Cathaysian lithosphere and tectonic evolution of the border sea basins in East Asia. Geochimica 31 (3), 213–221 in Chinese with English abstract.

Zhu, J.J., Qiu, X.L., Kopp, H.D., Xu, H.L., Sun, Z.X., Ruan, A.G., Sun, J.L., Wei, X.D., 2012. Shallow anatomy of a continent–ocean transition zone in the northern South China Sea from multichannel seismic data. Tectonophysics 554-557, 18–29.

Zou, H.B., Fan, Q.C., 2010. U-Th isotopes in Hainan basalts: implications for subasthenospheric origin of EM2 mantle endmember and the dynamics of melting beneath Hainan Island. Lithos 2010, 116,145–152.

Zou, H.B., Zindler, A., Xu, X.S., Qi, Q., 2000. Major, trace element, and Nd, Sr and Pb isotope studies of Cenozoic basalts in SE China: mantle sources, regional variations, and tectonic significance. Chem. Geol. 171 (1–2), 33–47.

Zou, H.B., Reid, M.R., Liu, Y.S., Yao, Y.P., Xu, X.S., Fan, Q.C., 2003. Constraints on the origin of historic potassic basalts from Northeast China by U-Th disequilibrium data. Chem. Geol. 200, 189–201.

Zou, H.P., Zhang, K., Liu, Y.L., Li, G., 2010. Geochemical characteristics and their geological implications of Meso-Cenozoic basalts in the Northern Ordos Block, North China. Geotecton. Metallog. 34 (1), 92–104 (in Chinese with English abstract).